LncRNA IMFlnc1 promotes porcine intramuscular adipocyte differentiation by sponging miR-199a-5p to up-regulate CAV-1

Jing Wang (12404634@qq.com)
Henan Academy of Agricultural Sciences https://orcid.org/0000-0001-8170-5835
Junfeng Chen
Henan Academy of Agricultural Sciences
Mingyue Chen
Northwest Agriculture and Forestry University
Liushuai Hua
Henan Academy of Agricultural Sciences
Qiaoling Ren
Henan Academy of Agricultural Sciences
Jiaqing Zhang
Henan Academy of Agricultural Sciences
Hai Cao
Henan Xing Rui agriculture and husbandry techonology
Xianxiao Bai
Henan Academy of Agricultural Sciences
Chuanying Pan
Northwest A&F university
Baosong Xing
Henan Academy of Agricultural Sciences

Research

Keywords: lncRNA, ceRNA, intramuscular adipocyte differentiation, miR-199a-5p, CAV-1

Posted Date: May 4th, 2020

DOI: https://doi.org/10.21203/rs.3.rs-25510/v1

Abstract

Background Local Chinese local pig breeds have better meat quality, such as thinner muscle fiber and higher intramuscular-fat (IMF) content. However, its molecular regulation mechanism has not been discussed in-depth. Studies indicated that long non coding RNAs (lncRNAs) participate in the regulation of muscle and fat development. The expressional differences of lncRNAs in the longissimus dorsi (LD) muscle were identified between Huainan pigs (local Chinese pigs, fat-type, HN) and Large White pigs (lean-type, LW) at 38, 58, and 78 days post conception (dpc).

Results In total, 2131 novel lncRNAs were identified in 18 samples, and 291, 305, and 683 differentially expressed lncRNAs (DELs) were found between these two breeds at three stages, respectively. GO and KEGG analysis of the DEL co expressed mRNAs showed that muscle development and energy metabolism were more active at 58 dpc in HN, but at 78 dpc in LW pigs. Muscle cell differentiation and myofibril assembly might contribute to earlier myogenesis and primary-muscle-fiber assembly in HN, and cell proliferation, insulin, and the mitogen-activated protein kinase (MAPK) pathway might contribute to longer proliferation in LW pigs. The PI3K/Akt and cAMP pathways were associated with higher IMF deposition in HN. IMFlnc1 was selected for functional verification, and results indicated that it regulated the expressional level of caveolin-1 (*CAV-1*) as a competing endogenous RNA (ceRNA) for miR-199a-5p.

Conclusion Our data contributed to understanding lncRNAs in porcine-muscle development and IMF deposition, and provided valuable information for improving pig-meat quality.

Background

Pork is the main source of animal protein in daily human diet, especially in China, where pork is consumed the most by residents. With the improvement of people's living standards, the quality of pork has received increasing amounts of attention. The diameter of muscle fibers, the content of intramuscular fat, and muscle fiber types are all involved in regulating meat-quality traits. Meat-quality traits are also regulated by nutrition, feeding conditions, stress, and, most importantly, by genetic influence. Lean-type pigs like Large White (LW), Landrace (LR), and Duroc generally have advantages such as high meat production, a fast growth rate, and a low feed-to-meat ratio. Most local Chinese pig breeds are fat-type, and they generally have bright red meat, thin muscle fibers, high intramuscular fat content, and more glycolytic muscle fibers. Two pig types with differences in meat-quality traits were a potentially good model to study the genetic-regulation mechanism of potential muscle-phenotype differences.

In recent years, there have been some studies focused on the differences between lean and fat-type pigs. The transcriptional profiling of the longissimus dorsi (LD) muscle from German Landrace (more obese) and Pietrain (more leaner) fetuses at 35, 63, and 91 days post conception (dpc) and adult pigs (180 days postnatal) was compared, and results indicated that the differential expression patterns were associated with muscle development stages and breed types[1]. Xu et al. compared the transcriptome of LD muscle between Northeast Min (fat-type) and Changbaishan (lean-type) wild boar at the age of 42 days; 4522 differentially expressed genes (DEGs) were mainly enriched in myofiber development, differentiation, growth, lipogenesis, and lipolysis[2]. The miRNAomes of LD muscle from LW and Meishan (MS) pigs at 35 dpc were compared, and results revealed that, in 87 differentially expressed miRNAs mainly enriched in muscle contraction, wingless/integrated (WNT), mammalian target of rapamycin (mTOR), mitogen-activated protein kinase (MAPK) signaling pathway, miR-133, miR-1, miR-206 and miR-148a were highly abundant in MS pigs, while the let-7 family, miR-214, and miR-181 were highly expressed in LW[3]. At postnatal day 240, 106 differentially expressed miRNAs were identified from the LD muscle of LR and Tongcheng (TC) pigs, and they were mainly enriched in the biological processes of oxidative stress and muscle-organ development[4]. Sun et al., compared the transcriptome of LD muscle between LR and Lantang (LT) pigs at the age of 7 days. They found 547, 5566, and 4360 differentially expressed mRNAs, lncRNAs, and circRNAs, respectively, and constructed 26 ceRNA interactions[5]. DNA methylation, mRNA, lncRNA and miRNA profiles in the LD muscle of TC, LR and Wuzhishan (WZS) pigs at the age of 240 days were compared, and differentially methylated genes were associated with lipid metabolism, oxidative stress, muscle development, and the p38 MAPK signaling pathway[6]. Differences in meat quality between fat- and lean-type pigs were mainly due to muscle development and lipid metabolism, and mRNA, miRNA, lncRNA, circRNA, and methylation were all involved in the regulation of meat quality.

In previous studies, LD muscle samples were collected from fetal, new-born, or adult pigs. Zhao et al., identified the characterization of large intergenic noncoding RNAs (lincRNAs) in the LD muscle of TC pigs at 50, 55, 60, 65, and 75 dpc[7], but the expressional

differences of lncRNAs during the embryonic stage between fat- and lean-type have not been systematic studied. During the embryonic stage, there are two major waves of fiber generation. The first wave is myoblasts differentiating into primary myofibers (35—60 dpc), and the second is the secondary myofibers forming a base on primary myofibers (54—90 dpc) [8, 9]. The total number of fibers (TNF) is fixed before birth, for postnatal development of skeletal muscle growth and maturation, so the embryonic stage plays an important role in skeletal muscle development [10, 11]. Existing studies showed that, during embryonic stages, there are significant differences in the development of muscle fibers between fat- and lean-type pigs [8, 12]. Researches also showed that adipogenic differentiation and the second wave of fiber generation are simultaneous in cattle. In the later stages of embryonic development, there were significant differences in intramuscular fat between TC and Yorkshire (YK) pigs [8]. In production, increasing the nutritional level of females in later pregnancy could promote muscle fat content of the young animals. Therefore, the embryonic stage is a key stage for studying meat quality traits.

As an excellent local breed in China, Huainan (HN) pigs are mainly distributed in the upper reaches of the Huai river, showing heat- and roughage-resistance, a larger litter size, and particularly high fat deposition. Huainan pigs were included in “fine livestock and poultry breeds in Henan province” in 1986 [13]. Previously, we studied the characterization of lncRNA in adult porcine subcutaneous fat and LD muscle [14–16]. So far, there are few studies on the regulation of lncRNAs on the muscle development in the embryo stage of Huainan pigs. In this study, considering the temporality of myogenic differentiation, we compared lncRNA expressional profiles in LD muscle between HN pigs and LW pigs at 38, 58, and 78 dpc. lnc_000167, one of the 37 shared differentially expressed lncRNAs (DELs) in different stages, was selected for functional verification, and it was named intramuscular fat deposition-associated long noncoding RNA 1 (IMFlnc1). Results were helpful to analyze the lncRNAs’ regulation mechanism on differences of meat quality between fat- and lean-type pigs during the embryonic period, and provide basic materials for improving meat quality traits for breeding.

Methods

Animals and tissue collection

Five HN and five LW sows (in their second or third parity) with the same genetic background were artificially inseminated with semen from the boars of the same breed. One sow from each breed was slaughtered at 38, 58, or 78 days of pregnancy. Fetuses were immediately taken out of the uteri, and three males and three females were selected. For 38 dpc, all of the fetuses were selected, and their sex were subsequently identified by the SRY gene. LD muscle tissue from the same area was obtained from the embryos and snap-frozen in liquid nitrogen. All pigs were raised under the same feeding and management practices [17] at Henan Xing Rui Agricultural and Animal Husbandry Technology Co., Ltd., Henan province, China.

Rna Isolation, Library Preparation, And Sequencing

Total RNA from LD muscle tissue was extracted by using TRIzol reagent (Invitrogen, USA) according to the manufacturer’s protocols. The NanoDrop spectrophotometer (Nano-Drop Technologies, USA) and Agilent 2100 Bioanalyzer (Agilent Technologies, USA) were used to detect the integrity, purity, and quality of the isolated RNA. Samples with an RNA integrity number (RIN) value larger than eight were used for library construction. DNase (QIAGEN, USA) and Ribo-Zero™ rRNA Removal Kit (Epicentre, USA) were used to remove residual genomic DNA and ribosomal RNA, respectively. Illumina TruSeq™ RNA Sample Prep Kit was used to construct the RNA sequencing library. Agilent 2100 Bioanalyzer (Agilent Technologies, USA) was used to analyze the libraries’ quality. The libraries were sequenced on an Illumina Hiseq 2500 platform, and 125 bp paired-end reads were generated. TopHat2 software was used to map the clean data to the porcine reference genome (Sscrofa 10.2, ftp://ftp.ensembl.org/pub/release-84/fasta/sus_scrofa/dna/) [18].

Identification Of Lncrnas And Differential Expression Analysis

The identification of lncRNAs followed these five steps: (1) transcripts that contained a single exon were removed; (2) transcripts shorter than 200 bp were removed; (3) annotated lncRNAs in the database that overlapped with the transcripts in this research were left as annotation lncRNAs for subsequent analysis (Cuffcompare software); (4) transcripts with FPKM ≤ 0.5 were removed;(5) the

coding potential of the transcripts was analyzed by Coding Potential Calculator (CPC, score < 0), Coding-Non-Coding-Index (CNCI, score < 0), Pfam (E value < 0.001), and k-mer scheme (PLEK, score < 0) software. Transcripts that passed all these software tests were considered lncRNAs.

GO and KEGG pathway analysis

Differentially the expressed lncRNAs (p_{adj} < 0.05 and |$\log_2$FoldChange|>0.3) were identified by the DESeq software package (http://bioconductor.org/packages/release/ bioc/html/DESeq.html). Gene ontology enrichment analysis of co-expressed mRNAs of DELs was performed by GOseq [19]. KEGG analysis was performed using KOBAS [20].

Validation Of Gene Expression In Rna-seq

To verify the accuracy of high-throughput sequencing results, ten lncRNAs were selected from the 37 shared DELs, and their expressional trends at 78 dpc between HN and LW pigs were validated by RT-qPCR. The RNA used in RT-qPCR was the same as that used in Illumina sequencing. PrimeScript RT reagent Kit with the gDNA Eraser (TaKaRa, China) was used to convert total RNA to cDNA [21]. Then, qPCR was performed using the SYBR Green PCR kit (TaKaRa, China) according the manufacturer's instructions. Each qPCR reaction was performed in a 20 μL reaction mixture, including 20 ng template cDNA, 10 μL 2 × SYBR Premix Ex Taq™, and 10 μM forward and reverses primers (Additional Table 1). PCR amplification included an initial denaturation step (95 ^{o}C for 30 s), and 40 cycles of 5 s at 95 ^{o}C and 34 s at 60 ^{o}C. Each qPCR experiment was performed in triplicate, and the relative RNA expression values were calculated using the $2^{-\triangle\triangle Ct}$ method [22], data are presented as fold changes in expression.

Table 1
The differently expressed lncRNAs between different libraries

Signaling pathway	H58/H38	LW58/LW38	H78/H58	LW78/LW58	H38/LW38	H58/LW58	H78/LW78
Insulin	↑	↑	↑	↑	↓	↓	↓
Calcium	↑	↑	↑	↑	↓	↓	↓
cAMP	↑	↑		↑	↓	↓	↓
HIF-1	↑	↑	↑	↑	↓	↑	↓
Fatty acid elongation	↑	↑	↑	↑	↓		
Glycolysis/gluconeogenesis	↑	↑	↑	↑			↓
Glyoxylate and dicarboxylated metabolism	↑	↑		↑			↓
MAPK	↑	↑				↓	↓
Fatty acid degradation	↑		↑	↑	↓		↓
Biosynthesis of unsaturated fatty acid	↓	↓	↓	↓	↑↓	↓	
Metabolic pathways	↓	↓		↓			
Cardiac muscle contraction	↑	↑	↑	↑		↑↓	↓
cGMP-PKG	↑	↑	↑	↑	↓	↑↓	
Type II diabetes mellitus	↑↓	↑↓	↑	↑	↓	↓	
HCM	↑↓	↑↓	↑	↑	↑↓	↑↓	↓
ARVC	↑↓	↑↓	↑	↑↓	↑↓	↓	↑↓
Biosynthesis of amino acids	↑↓	↑	↑	↑	↑↓	↑	↓
Insulin secretion	↑	↑↓	↑	↑	↓	↓	↑
Adipocytokine pathway	↑	↓	↑	↑↓	↓	↑	↓
Focal adhesion	↑↓	↑↓	↑↓	↑↓	↑↓	↑↓	↑↓
PI3K-Akt	↑↓	↑↓	↑↓	↑↓	↑↓	↑↓	↑
ECM-receptor interaction	↑↓	↑↓	↑↓	↑↓	↑↓	↑↓	↑
Steroid biosynthesis	↑↓	↑↓	↑↓	↑↓	↑↓	↑	↑
AMPK	↑↓	↑↓	↑↓	↑↓	↓	↓	↓
Fatty acid metabolism	↑↓	↑↓		↑↓	↑↓	↑	↓
Ala, asp and glu metabolism	↑↓	↑↓	↑		↑		↑↓
Arginine and proline metabolism	↑↓	↑↓		↑↓			↑↓
Carbon metabolism	↑↓	↑↓	↑	↑↓			↓
Fructose and mannose metabolism			↑	↑		↑	↓

Ala, asp and glu metabolism: Alanine, aspartate and glutamate metabolism; ↑: up-regulated;↓: down-regulated. ↑↓: up-regulated and down-regulated.

Signaling pathway	H58/H38	LW58/LW38	H78/H58	LW78/LW58	H38/LW38	H58/LW58	H78/LW78
Rap1	↑↓	↑↓	↑			↓	↑
Protein digestion and absorption				↑		↑	↑

Ala, asp and glu metabolism: Alanine, aspartate and glutamate metabolism; ↑: up-regulated;↓: down-regulated. ↑↓: up-regulated and down-regulated.

Construction Of Lncrna-mirna-mrna-pathway Regulatory Network

The interaction between the 37 shared DELs and miRNAs was analyzed by the miRanda software. MiRNAs came from the LD muscle of HN and LW pigs at 38, 58, and 78 dpc, and these data were not published. The construction of the network included three steps, and the methods were the same as those previously described [16].

Isolation, Differentiation, And Culture Of Porcine Intramuscular Adipocyte

Porcine intramuscular adipocyte were isolated from the LD muscle of HN pigs at 2 days of age following methods as previously described [23, 24]. Intramuscular adipocytes were cultured with the normal medium: DMEM/F12 supplemented with FBS (10%) and antibiotics (penicillin, 100 IU/mL; streptomycin, 100 μg/mL) at 37 °C and 5% CO_2 in a normal-atmosphere incubator. Two days after 100% confluence, cells were maintained with a differentiation medium (0.5 mM IBMX, 1 mM DEX, 5 μg/mL of insulin add to the “normal medium”). After two days, the medium was changed to a maintenance medium (5 μg/mL of insulin add to the “normal medium”) for two days. Then the medium was changed to the “normal medium”.

Rna Fluorescence In Situ Hybridization (rna Fish)

Cy3-labeled IMFlnc1 probes were obtained from RiboBio (Guangzhou, China). Fluorescent in situ hybridization kit was used to detect the subcellular localization of IMFlnc1.

Imflnc1 Knockdown

Interference of IMFlnc1 was conducted using a Ribo™ Smart Silencer, designed and synthesized in Ribobio (Guangzhou, China). When cultured primary intramuscular preadipocytes reached 70–80% confluence, smart silencer (25, 50, or 75 nM) or NC was transfected by DharaFect 2 according to the manufacturer’s instruction (Dharmacon, USA). Twelve hours later, cells were recovered in full culture media and grown to confluence; then, cells were induced to differentiate. Twenty-four hours after transfection, the cells were harvested for the detection of interference efficiency (primers showed in Additional Table 1). Six days after differentiation, cells were detected by Oil Red O staining.

Plasmid Construction

The full lengths of IMFlnc1 and 3’ UTR of *CAV-1* were cloned into the psiCHECK-2 vector (Promega, USA). The mutant IMFlnc1 and 3’ UTR of CAV-1 without the seed region of miR-199a-5p were generated by overlapping extension PCR. An miR-199a-5p sensor was generated by inserting two consecutive miR-199a-5p complementary sequences into psiCHECK-2.

Luciferase Assays

HEK293T cells were seeded in 48-well plates in triplicate, and plasmids were transfected when the cell reached 70% or 80% confluence. Forty-eight hours after transfection, luciferase activities were measured using the Dual-Luciferase Reporter Assay

System (Promega) on a Fluoroskan Ascent FL instrument (Thermo Fisher Scientific, USA). For each sample, renilla luciferase activity was normalized to firefly luciferase activity.

Statistical analysis

Results were expressed as the mean ± SE, and a *p* value of < 0.05 was considered statistically significant.

Results

lncRNA identification in porcine LD muscle

In order to study the function of lncRNAs in muscle development during porcine embryonic development, we examined the DELs of LD muscles between HN and LW pigs at the three embryonic-development stages. In total, 1.94 billion clean reads were obtained from 18 samples, of which 79.63% could be aligned to the reference porcine genome (Sscrofa10.2), 12.87% were multiply mapped, 66.76% were uniquely mapped, 33.34% mapped to "+", 33.47% mapped to "−", 19.24% were splice reads, and 47.52% was nonsplice reads (Additional Table.2). Expression correlation between the three samples in the same treatment was from 0.953 to 0.969 (Additional Fig. 1), indicating that sample selection was reasonable, and experiment results were reliable. Raw sequence data were submitted to the NCBI Sequence Read Archive under succession number SRP243554.

Lncrna Properties In Porcine Ld Muscle

In total, 2057 annotated lncRNAs and 2131 novel lncRNAs were obtained from 18 samples (Fig. 1a), and only lincRNA(89.9%)and intronic lncRNA were found in the novel lncRNAs (Fig. 1b). The average length of the annotated lncRNAs was shorter than that of the novel lncRNAs, but there was no significant difference in exon number and open reading frame (ORF) length (Fig. 1c). For the novel lncRNAs, the average length of antisense lncRNAs was longer than that of lincRNAs (Fig. 1d). Information on the novel lncRNAs is shown in Additional Table 3.

Expression Difference Of Lncrnas Between Hn And Lw Pigs

The fragments per kilobase per million (FPKM) of lncRNAs were lower than those of mRNAs (Fig. 2a), and the FPKM distribution of LW pigs at 78 dpc was higher than that of the others (Fig. 2b). Systematic cluster analysis was performed to compare the relationship between 18 LD muscle libraries, and results indicated that three replicates of the same sample were very conservative (Fig. 2c). The expression differences between the different stages were larger than those of the two breeds. There were 1155 and 751 DELs during muscle development in HN and LW pigs, respectively. In HN pigs, 579 and 809 DELs were identified at 58 vs 38 dpc and 78 vs 58 dpc, and 213 DELs were shared in these two comparisons. In LW pigs, there were 579 and 809 DELs at 58 vs 38 dpc and 78 vs 58 dpc, respectively, and 167 DELs were shared. At 78 vs 58 dpc, there were more DELs in HN than in LW pigs. There were 291, 305, and 683 DELs between these two breeds at 38, 58, and 78 dpc, and 37 DELs were shared by these three stages (Fig. 2d and Additional Fig. 2 and Additional Table 4).

During embryonic muscle development, the GO enrichment of DEL-co-expressed genes in HN showed that skeletal muscle tissue/organ development, muscle organ development, striated muscle tissue development, as well as the response to oxygen-containing compound were upregulated in 58 dpc. In LW pigs, only the response to the oxygen-containing compound upregulated at 58 dpc, and muscle cell differentiation, myofibril assembly only upregulated at 78 dpc; other muscle development-related pathways were continuously upregulated in both breeds. At 58 vs 38 dpc, muscle cell differentiation and myofibril assembly were only upregulated in HN at 58 dpc. Skeletal muscle tissue/organ development, muscle organ development, striated muscle tissue development was only upregulated in LW at 78 dpc (Table 1).

KEGG enrichment of DEL-co-expressed genes shown that the cyclic adenosine monophosphate (cAMP), glyoxylate and dicarboxylated metabolism, metabolic pathways were only upregulated in HN pigs at 58 dpc. Fatty acid degradation and fructose and mannose metabolism was only upregulated in LW pigs at 78 dpc. The adipocytokine pathway was upregulated in HN but downregulated in LW pigs at 58 dpc. The MAPK pathway was upregulated only at 58 dpc in both breeds, and fructose and

mannose metabolism was upregulated only at 78 dpc in both breeds. DEL-co-expressed genes related to fatty acid degradation, cAMP, glyoxylate and dicarboxylated metabolism, fatty acid metabolism, metabolic pathways continuously changed only in HN or LW pigs. Genes associated with alanine, aspartate and glutamate metabolism, and Rap1 were higher expressed only in HN pigs at 78 dpc, while genes in protein digestion and absorption were expressed at a higher level in LW pigs at 78 dpc (Table 2 and Additional Fig. 3).

Table 2
The muscle-related GO terms of DELs co-expressed genes during muscle development stages in Huainan and Large white pigs

GO terms	H58/H38	LW58/LW38	H78/H58	LW78/LW58	H58/LW58	H78/LW78
muscle cell differentiation	↑ 9 (0.260)		↑ 9 (0.241)	↑10 (0.062)	↑ 6 (0.438)	↓ 6 (0.868)
contractile fiber	↑ 8 (0.065)	↑ 7 (0.180)	↑ 8 (0.084)	↑ 8 (0.011)	↑ 5 (0.361)	
myofibril	↑ 7 (0.089)	↑ 6 (0.268)	↑ 7 (0.106)	↑ 7 (0.027)	↑ 4 (0.415)	
regulation of glucose metabolic process	↑ 5 (0.124)	↑ 5 (0.227)	↑ 5 (0.163)	↑ 5 (0.046)	↑ 3 (0.480)	
muscle structure development	↑12 (0.157)	↑11 (0.278)	↑12 (0.174)	↑13 (0.029)	↑ 8 (0.385)	
muscle system process	↑ 9 (0.160)	↑ 8 (0.278)	↑ 6 (0.247)	↑ 9 (0.061)	↑ 6 (0.385)	
muscle tissue development	↑11 (0.148)	↑10 (0.278)	↑10 (0.212)	↑13 (0.011)		↓ 7 (0.757)
skeletal muscle tissue development	↑ 8 (0.160)	↑ 8 (0.240)		↑10 (0.011)	↑ 5 (0.415)	↓ 5 (0.778)
skeletal muscle organ development	↑ 8 (0.161)	↑ 8 (0.260)		↑10 (0.011)	↑ 5 (0.438)	↓ 5 (0.847)
muscle organ development	↑10 (0.180)	↑ 9 (0.312)		↑12 (0.013)	↑ 6 (0.480)	↓ 7 (0.608)
myofibril assembly	↑ 4 (0.124)		↑ 4 (0.163)	↑ 4 (0.046)		↓ 3 (0.544)
striated muscle tissue development	↑10 (0.180)	↑ 9 (0.334)		↑12 (0.015)		↓ 7 (0.608)
response to oxygen-containing compound	↑19 (0.124)	↑19 (0.179)				
cell proliferation				↑20 (0.195)		↓16 (0.544)

The results of GO enrichment of DELs between HN and LW pigs at the same stage showed that no pathway was enriched between these two breeds at 38 dpc. At 58 dpc, genes in muscle cell differentiation and eight other pathways had a higher expression level in HN pigs. At 78 dpc, the genes in seven pathways were downregulated in HN pigs. Compared with LW pigs, the genes associated with muscle cell differentiation, skeletal muscle tissue/organ development, muscle organ development pathways showed, higher expressional level at 58 dpc, but a lower expression level in HN pigs (Table 1 and Additional Table 4).

KEGG analysis indicated that DEL-co-expressed genes involved in insulin, calcium, and the cAMP signaling pathway were continuously highly expressed in HN pigs. Genes in steroid biosynthesis were expressed at a higher level in HN pigs at 58 and 78 dpc. Compared with LW pigs, genes in hypoxia-inducible factor 1 (HIF-1) and adipocytokine were upregulated in LW pigs at 38 and 78 dpc, but downregulated at 58 dpc. Genes involved in insulin secretion and Rap1 were downregulated at 58 dpc and upregulated at 78 dpc in HN pigs. The expression trends of genes in the biosynthesis of amino acids, fatty acid metabolism, and fructose and mannose metabolism were completely opposite (Table 2 and Additional Fig. 3).

Potential Function Of Dels

The expressional level of 37 shared DELs between these two breeds at three stages are shown in Fig. 3a, b. The ceRNA regulatory network of these shared DELs was constructed and visualized using Cytoscape software, including 30 lncRNAs, 27 miRNAs, 27 mRNAs, and 24 pathways (Fig. 3c). LncRNAs had up to 7 interacting miRNAs, such as ALDBSSCT0000006192, and miR-199a-5p had the most target lncRNAs, seventeen target lncRNAs for each miRNA. Considering the abundance and transcript length, IMFlnc1 was selected for subsequent verification among miR-199a-5p target lncRNAs. IMFlnc1 is located on porcine chromosome 7, and includes two exons.

Imflnc1 Inhibits Adipogenesis Of Intramuscular Adipocytes

RT-qPCR showed that IMFlnc1 is expressed at the highest level in the gut and lungs, followed by in intermuscular fat. Its expression level in subcutaneous fat was lower than it was in intermuscular fat, but higher than it was in LD muscle (Fig. 4a). Moreover, time-course analysis showed that the expression level of IMFlnc1 was upregulated during porcine intramuscular preadipocyte differentiation (Fig. 4b).

CPC software showed that IMFlnc1 has very low coding potential, similar to ADNCR [25], a well-known lncRNA (Fig. 4c). To explore the function of IMFlnc1 in adipogenesis, we performed knockdown IMFlnc1 in intramuscular adipocytes by lncRNA smart silencer, which significantly reduced its RNA level by 60%, and the expression of CAV-1 and adipogenic markers PPARgama decreased significantly (Fig. 4d). Oil O staining indicated that the knockdown of IMFlnc1 inhibited adipogenesis (Fig. 4e).

Imflnc1 And Cav-1 Were Target Genes Of Mir-199a-5p

RNA FISH indicated that IMFlnc1 is predominantly localized in the cytoplasm of preadipocytes (Fig. 5a), so it might participate in the regulation of adipogenesis through ceRNA mechanism. The IMFlnc1-miR-199a-5p-CAV-1 pathway was selected from the ceRNA network to verify its function in adipogenesis. Bioinformatics analysis of the RNAhybrid showed that there exists a putative miR-199a-5p binding site in IMFlnc1 and CAV-1 (Fig. 5b), and the binding site in *CAV-1* is conservative in different animals (Fig. 5c). RT-qPCR results showed that the expression of IMFlnc1 and *CAV-1* has a positive correlation in porcine LD muscle (Fig. 5d, $R^2 = 0.590$).

Luciferase assay indicated that miR-199a-5p significantly reduced the Rluc activity of the miR-199a-5p sensor and psiCHECK2-IMFlnc1 ($p < 0.01$, Fig. 5e), but the reduction of the miR-199a-5p sensor was higher than the reduction of psiCHECK2-IMFlnc1. However, miR-199a-5p had no effect on the fluorescence activity of psiCHECK2-IMFlnc1-Mut, which indicated that IMFlnc1 was the target gene of miR-199a-5p. Similarly, luciferase assay proved that *CAV-1* was the target gene of miR-199a-5p (Fig. 5f).

IMFlnc1 participates in adipogenesis by increasing *CAV-1* in miR-199a-5p-dependent manner

To verify whether IMFlnc1 might act as the sponge of miR-199a-5p, the miR-199a-5p sensor was transfected with pcDNA3.1+, pcDNA-miR-199a-5p or pcDNA-miR-199a-5p and pcDNA-IMFlnc1. The Rluc activity of the miR-199a-5p sensor was significantly reduced by pcDNA-miR-199a-5p ($P < 0.01$), but IMFlnc1 recovered the Rluc activity in a dose-dependent manner ($P < 0.01$, Fig. 5g). However, pcDNA-IMFlnc1-Mut, in which the binding site of miR-199a-5p was mutated, no longer elicited such an effect. These results indicated that IMFlnc1 act as a ceRNA for miR-199a-5p.

As shown in Fig. 4d, h, the mRNA expression of CAV-1 was reduced during the reduction of IMFlnc1. To further determine whether IMFlnc1 regulated *CAV-1* through miR-199a-5p, psiCH2-CAV-1 was co-transfected with pcDNA3.1, pcDNA-IMFlnc1 or pcDNA-IMFlnc1Mut, respectively. The Rluc activity of *CAV-1* was improved by the overexpression of IMFlnc1, but the overexpression of IMFlnc1 with the mutated miR-199a-5p binding sites no longer elicited similar effect (Fig. 5h). In summary, these results indicated that IMFlnc1 might promote adipogenesis by acting as a ceRNA for miR-199a-5p to regulate *CAV-1* expression.

Discussion

Previous studies showed that muscle development during the embryonic stages is different between lean- and fat-type pigs. The morphological differences of LD muscle between LT and LR pigs were compared by histological section, and results showed that a few primary fibers were present at 35 dpc in LT pigs, but 49 dpc in LR pigs. At 63 dpc, the secondary fibers were formed in both breeds, but LR pigs had more fibers and larger muscle fiber diameter at 91 dpc [12]. Zhao et al., compared the morphological differences of muscle between TC and YK pigs, the number and density of myoblasts in TC was more than that in YK pigs at 30 dpc, primary fibers could be found at 40 dpc in both breeds, and the secondary fibers appeared at 55 dpc in YK pigs but later in TC pigs [8]. These studies indicated that myoblast differentiation, the formation of primary fibers and secondary fibers, and muscle fiber diameter was different between fat- and lean-type pigs. To study the regulation of lncRNA in meat quality between the fat- and lean-type pigs, differentially expressed lncRNAs in LD muscle between HN and LW pigs at 38, 58, and 78 dpc were identified. Results indicated that there were more DELs in 58 vs 38 dpc than in 78 vs 58 dpc in HN pigs. However, there was the completely opposite trend in LW pigs. These coincided with the difference in muscle fibers development between fat- and lean-type pigs.

GO analysis of DEL-co-expressed genes was performed to further understand their biological functions (Table 1), and results showed that DELs related to muscle structure/tissue/system development were continuously upregulated in both breeds, with higher expression at 58 dpc, but lower expression at 78 dpc in HN pigs compared to that in LW pigs. Muscle cell differentiation was continuously upregulated in HN pigs, but only upregulated at 78 dpc in LW pigs, and with a higher expressional level at 58 dpc, but lower at 78 dpc in HN than in LW pigs. Similarly, contractile fiber and myofibril were continuously upregulated in both breeds, but at 58 dpc their expression was higher in HN than in LW pigs. Genes in the myofibril assembly pathway were continuously upregulated in HN pigs, but upregulated only at 78 dpc in LW pigs, and its expressional level at 78 dpc were higher in LW pigs. These results indicated that compared with LW pigs, HN pigs showed earlier myogenic differentiation. Muscle development-related biological activities were most active at 58 dpc in HN pigs, but most active at 78 in LW pigs.

To identify pathways in muscle development, DEL-co-expressed genes were mapped to the reference canonical pathways in the KEGG database (Table 2). Hypoxia inducible factor-1α (HIF-1α), a key pathway regulating myogenic differentiation, showed higher expression at 58 dpc, but lower expression at 78 dpc in HN than in LW pigs. The pathways associated with energy metabolism showed the same trends, such as biosynthesis of amino acids, adipocytokine pathway, fatty acid metabolism, and fructose and mannose metabolism. These results verified that myogenic differentiation in HN pigs was most active at 58 dpc, so more energy is needed at this period. In contrast, LW pigs showed the most active myogenic differentiation at 78 dpc, so energy-related genes had higher expression at 78 dpc.

Previous researchers found that the myoblast proliferation phases of LD in TC pigs were longer than that those in WZS pigs [4], and it was predicted that cell proliferation may contribute to differences in muscle mass and body size between these two breeds [6]. In the current study, GO analysis showed that cell proliferation was at a higher level in LW than in HN pigs at 78 dpc. The insulin [26] and the MAPK [27] pathways both promote muscle cell proliferation. The insulin pathway showed a higher expressional level in LW than that in HN pigs in all three stages. MAPK showed a higher level in LW than in HN pigs at 58 and 78 dpc. These results verified that myoblast proliferation was higher in LW than in HN pigs, which coincided with more muscle mass in LW pigs.

It was reported that phosphatidylinositol-3- kinases/protein-serine-threonine kinase (PI3K/Akt) participates in the adipogenic differentiation of mesenchymal stem cells [28]. The proliferation and differentiation of porcine intramuscular preadipocytes are activated by G protein-coupled receptor (GPR) 39 through the PI3K/Akt cell signaling pathway [29]. In this research, PI3K/Akt was expressed at a higher level in HN pigs at 78 dpc. The cAMP pathway, which could inhibit adipocyte differentiation and promote lipolysis [30], was continuously downregulated at the prenatal period in both breeds, but its expressional level was lower in HN than in LW pigs in all three stages. These results coincided with the higher IMF content in HN pigs.

The GO and KEGG results of DELs were consistent with previous studies on the differences in embryonic muscle development between fat- and lean-type pigs. To explore how these DELs participated in the regulation of muscle development, interactions between the 37 shared DELs and miRNAs were analyzed by miRanda software. As shown in Fig. 4c, miRNAs enriched in the ceRNA network were associated with meat quality. The expression of miR-125, miR-133, and miR-199 in LD muscle was significantly different between German Landrace and Pietrain (Pi) pig breeds at the pre- and post-natal period [31]. Similarly, miR-133 was significantly highly abundant in MS (fat-type) than that in LW (lean-type) pigs at all prenatal stages (35, 55, and 90 dpc) [32]. The

expression of miR-199, miR-423, miR-296, miR-193 and miR-125 was significantly different between castrated male pigs (with more fat deposition) and intact male pigs (with less fat deposition) [33]. MiR-423-5p was increased in the plasma of obese children [34]. The expression of miR-342, miR-193a-3p, miR-365 and miR-125 was significantly different between obese and lean individuals [35].

There were also muscle-development-related miRNAs in the ceRNA network, such as miR-133, which was significantly more highly expressed in MS pigs skeletal muscle compared with that in LW pigs at all prenatal stages [32]. SNPs in miR-133 were significantly associated with total muscle fiber number, loin eye area, and muscle pH [36]. Meanwhile, it was reported that miR-133 could promote myoblast differentiation and inhibit proliferation through the extracellular signal-regulated kinase (ERK) signaling pathway [37]. It also participates in the regulation of the metabolic difference between glycolytic and oxidative myofibers [38]. MiR-365 could inhibit myoblast proliferation by targeting insulin-like growth factor I (IGF-I) or cyclinD1 [39–41]. MiR-125 regulates muscle differentiation by target myocyte-specific enhancer factor 2D (Mef2d) [42, 43].

There are also several miRNAs associated with lipid metabolism in the ceRNA network, for example, miR-370 repressed lipid accumulation in porcine adipocytes [44]. MiR-326 reduced adipogenic differentiation by targeting CCAAT enhancer binding protein-α (C/EBPα) [45]. It was reported that miR-574-5p regulates white adipocytes hypertrophy by targeting early B cell factor 1 (EBF1) [46]. MiR-296 participated in lipoapoptosis regulation by reducing PUMA (also known as BCL2 binding component 3) [47]. The expressional level of miR-874 was lower in Wagyu (high intramuscular fat) than that in Holstein (moderate intramuscular fat) cattle [48].

In the ceRNA network there are the miRNAs associated not only with muscle development, but also with adipocyte development, such as miR-199a-5p, which has the most targets in the current ceRNA network. As the key regulator in the Wnt signaling pathway, miR-199a-5p induced muscle proliferation by targeting HIF-1, which is the key regulator in smooth muscle hypertrophy [49–51]. It also regulates cardiomyocyte apoptosis by targeting JunB (JunB proto-oncogene) [52]. In diabetic individuals, miR-199a-5p may be involved in skeletal muscle insulin resistance by inhibiting glucose transporter 4 (GLUT4) and hexokinase 2 (HK2) [53]. MiR-199a-5p also participates in lipid metabolism. In Italian Large White pigs, miR-199a-5p showed a lower expressional level in the backfat of the lean groups than that in the fat group [54]. Its expressional level was also higher in undifferentiated 3T3-L1 adipocytes, and rapidly reduced during differentiation [55]. Overexpression of miR-199a-5p in human bone-marrow-derived mesenchymal stem cells, the marker gene of adipocytes-FABP4 (ap2) was inhibited [56]. In mice, groin fat pads weight was reduced when the Dnm3os (DNM3 opposite strand/antisense RNA) was knocked down, which served as a precursor of miR-199a-5p and miR-199a-3p [57]. In porcine preadipocytes, miR-199a-5p significantly promotes proliferation, and reduced adipogenesis by targeting *CAV-1* [58]. MiR-199a-5p could be regulated by *PPARgama* in a transcription-independent manner, and it regulates adipogenic differentiation by targeting the expression of transforming growth factor beta induced (TGFBI) [59]. In general, miR-199a-5p was not only associated with the proliferation and differentiation of muscle cells, but also with the proliferation and adipogenesis of pre-adipocytes. Similarly, miR-370 was not only related to lipid metabolic homeostasis and lipid deposition,[44] but it also regulates muscle cell apoptosis [60]. MiR-149 promoted porcine satellite cell proliferation through the Notch signaling pathway [61], while miR-149-3p induced a subcutaneous-to-visceral fat switch by suppressing PR domain-containing 16 (PRDM16) [62].

There are several coding genes associated with meat quality, such as adipocyte determination and differentiation dependent factor 1 (ADD1), which stimulates PPARgama expression and plays an important role in adipogenic differentiation [63], whose expressional level is positively correlated with IMF content ($P < 0.05$) [64], The stearoyl-CoA desaturase (SCD) gene plays a key role in the desaturation of fatty acids and synthesis of oleic fatty acid, and SCD overexpression in muscle is correlated with a higher IMF content [65]. SCD showed a significantly different expressional level in LD muscle between LT and LR pigs [66]. IGF-I regulates myofiber hypertrophy postnatally through the PI3K-Akt-mTOR pathway, which increased skeletal muscle mass in economic livestock, while IGF-I promotes free fatty acid oxidation and improves insulin sensitivity in muscle [67]. As a major fatty acid binding protein in adipocytes, CAV-1 moves from the plasma membrane to lipid droplets under the action of free fatty acids [68, 69]. Compared with Large YK pigs, CAV-1 showed a significantly higher expressional level in the backfat($P < 0.01$)and longissimus dorsi muscle（$P < 0.05$）in LT [70]. CAV-1-deficient mice showed a lean body phenotype, insulin resistance, and hypertriglyceridemia with adipocyte abnormalities [71]. Activated by TNF-α, CAV-1 reduces 3T3-L1 cell differentiation and blocks insulin-mediated glucose uptake [72]. CAV-1 was associated with lipoprotein metabolism [73], lipolysis [73], cholesterol homeostasis [74], fatty acid intake [75], and atherosclerosis [76], so CAV-1 is an important regulator of adipogenic differentiation and glycolipid metabolism.

These muscle development and lipid metabolism related coding genes and miRNAs in the ceRNA network indicated that these DELs may participate in the regulation of meat quality via the ceRNA mechanism. So, the miR-199a-5p-IMFlnc1-CAV-1 pathway was selected to be verified in porcine intramuscular adipocytes (Figs. 4 and 5). The results indicated that IMFlnc1 had broad-spectrum expression in different tissue types, and its expressional level was upregulated during the differentiation of intramuscular preadipocytes. Oil red O staining suggested that the reduction of IMFlnc1 inhibits adipogenesis. Luciferase assay revealed that IMFlnc1 could function as a ceRNA that sequesters miR-199a-5p, thereby protecting CAV-1 transcripts from miR-199a-5p-mediated suppression. At the same time, miR-199a-5p also participated in the regulation of myoblast differentiation. The role of IMFlnc1 in muscle cell proliferation and differentiation could be verified in further research.

Conclusion

In summary, a genome-wide view of the expression profiling of lncRNAs in pocine LD muscle at 38, 58, and 78 dpc between HN and LW pigs was investigated. These findings were of great significance for understanding the molecular regulation mechanisms of meat quality trait differences between fat- and lean-type pigs.

Abbreviations

ADD1:adipocyte determination and differentiation dependent factor 1; cAMP: cyclic adenosine monophosphate; CAV-1: caveolin-1; C/EBPα: CCAAT enhancer binding protein-α; ceRNA: competing endogenous RNA; CNCI: Coding-Non-Coding-Index; CPC: Coding Potential Calculator; DEGs: differentially expressed genes; DELs: differentially expressed lncRNAs; Dnm3os: DNM3 opposite strand/antisense RNA; dpc: days post conception; EBF1: early B cell factor 1; ERK: extracellular signal-regulated kinase; FABP4: fatty acid binding protein 4; FPKM: fragments per kilobase per million; GLUT4: glucose transporter 4; GO: Gene Ontology; GPR G: protein-coupled receptor; HIF-1α : hypoxia inducible factor-1α; HK2: hexokinase 2; HN: Huainan pigs; IGF-I : insulin-like growth factor I; IMF: intramuscular-fat; IMFlnc1: intramuscular fat deposition-associated long noncoding RNA 1; JunB: JunB proto-oncogene; KEGG: Kyoto Encyclopedia of Genes and Genomes; LD: longissimus dorsi; lincRNAs: large intergenic noncoding RNAs; lncRNAs: long non coding RNAs; LR: Landrace; LT: Lantang; LW: Large White; MAPK: mitogen-activated protein kinase; Mef2dL myocyte-specific enhancer factor 2D; MS: Meishan; mTOR: mammalian target of rapamycin; ORF: open reading frame; Pi: Pietrain; PI3K/Akt: phosphatidylinositol-3-kinases/protein-serine-threonine kinase; PRDM16: PR domain-containing 16; RIN: RNA integrity number; RNA FISH: RNA fluorescence in situ hybridization; SCD: stearoyl-CoA desaturase; TC: Tongcheng; TGFBI: transforming growth factor beta induced; TNF: total number of fibers; WNT: wingless/integrated; WZS: Wuzhishan; YK: Yorkshire; SCD: stearoyl-CoA desaturase; TC: Tongcheng; TGFBI: transforming growth factor beta induced; TNF: total number of fibers; WNT: wingless/integrated; WZS: Wuzhishan; YK: Yorkshire.

Declarations

Ethics approval

All procedures involving animals described in the present study were performed according to the procedures of Institutional Animal Care and Use Committee (IACUC), approved by the Institute of Animal Science of Henan Academy of Agricultural Sciences (code 7 Aug 2017). The pigs were allowed access to feed and water ad libitum under normal onditions, and all efforts were made to minimize their suffering.

Competing interests

The authors declare that they have no competing interests.

Fundings

This study was supported by the National Natural Science Foundation of China (31601927), Fund for Distinguished Young Scholars from the Henan Academy of Agricultural Sciences (2019JQ05), and Financial Budget Project of Henan Province, grant number 182102110063, 2017-76-15.

Author Contributions

J.W., C.P., and B.X. designed the study. J.W. and J.C. wrote the paper. H.C. collected the tissue samples. J.W. and M.C. performed most of the experiments. J.C., J.Z., L.H., and Q.R. carried out part of the experiments. J.C. and L.H. carried out data analyses. X.B. revised the manuscript. All authors contributed to drafting the manuscript. All authors have read and approved the final manuscript.

References

1. Siengdee P, Trakooljul N, Murani E, Schwerin M, Wimmers K, Ponsuksili S. Transcriptional profiling and miRNA-dependent regulatory network analysis of longissimus dorsi muscle during prenatal and adult stages in two distinct pig breeds. Anim Genet. 2013;44(4):398–407.
2. Xu XX, Mishra B, Qin N, Sun X, Zhang SM, Yang JZ, Xu RF. Differential Transcriptome Analysis of Early Postnatal Developing Longissimus Dorsi Muscle from Two Pig Breeds Characterized in Divergent Myofiber Traits and Fatness. Animal Biotechnol. 2019;30(1):63–74.
3. He DT, Zou TD, Gai XR, Ma JD, Li MZ, Huang ZQ, Chen DW. MicroRNA expression profiles differ between primary myofiber of lean and obese pig breeds. PloS one. 2017;12(7):e0181897–7.
4. Hou XH, Yang YY, Zhu SY, Hua CJ, Zhou R, Mu YL, Tang ZL, Li K. Comparison of skeletal muscle miRNA and mRNA profiles among three pig breeds. Molecular genetics genomics: MGG. 2016;291(2):559–73.
5. Sun JJ, Xie M, Huang Z, Li H, Chen T, Sun R, Wang J, Xi Q, Wu T, Zhang Y. Integrated analysis of non-coding RNA and mRNA expression profiles of 2 pig breeds differing in muscle traits. Journal of animal science. 2017;95(3):1092–103.
6. Yang YL, Liang GM, Niu GL, Zhang YY, Zhou R, Wang YF, Mu YL, Tang ZL, Li K. Comparative analysis of DNA methylome and transcriptome of skeletal muscle in lean-, obese-, and mini-type pigs. Sci Rep. 2017;7:39883–3.
7. Zhao WM, Mu YL, Ma L, Wang C, Tang ZL, Yang SL, Zhou R, Hu XJ, Li MH, Li K. Systematic identification and characterization of long intergenic non-coding RNAs in fetal porcine skeletal muscle development. Sci Rep. 2015;5:8957.
8. Zhao YQ, Li J, Liu HJ, Xi Y, Xue M, Liu WH, Zhuang ZH, Lei MG. Dynamic transcriptome profiles of skeletal muscle tissue across 11 developmental stages for both Tongcheng and Yorkshire pigs. BMC Genomics. 2015;16(1):377–7.
9. Picard B, Lefaucheur L, Berri C, Duclos MJ. Muscle fibre ontogenesis in farm animal species. Reprod Nutr Dev. 2002;42(5):415–31.
10. Ashmore CR, Addis PB, Doerr L. Development of muscle fibers in the fetal pig. Journal of animal science. 1973;36(6):1088–93.
11. Wigmore PM, Stickland NC. Muscle development in large and small pig fetuses. Journal of anatomy. 1983;137(Pt 2):235–45.
12. Zhao X, Mo DL, Li AN, Gong W, Xiao SQ, Zhang Y, Qin LM, Niu YN, Guo YX, Liu XH, Cong PQ, He ZY, Wang C, Li JQ, Chen YS. Comparative analyses by sequencing of transcriptomes during skeletal muscle development between pig breeds differing in muscle growth rate and fatness. PloS one. 2011;6(5):e19774–4.
13. Tao H, Mei SQ, Sun XJ, Peng XW, Zhang XY, Ma CP, Wang L, Hua L, Li FE. Associations of TCF12, CTNNAL1 and WNT10B gene polymorphisms with litter size in pigs. Anim Reprod Sci. 2013;140(3–4):189–94.
14. Wang J, Hua LS, Chen JF, Zhang JQ, Bai XX, Gao BW, Li CJ, Shi ZH, Sheng WD, Gao Y, Xing BS. Identification and characterization of long non-coding RNAs in subcutaneous adipose tissue from castrated and intact full-sib pair Huainan male pigs. BMC Genomics. 2017;18(1):542–2.
15. Xing BS, Bai XX, Guo HX, Chen JF, Hua LS, Zhang JQ, Ma Q, Ren QL, Wang HS, Wang J. Long non-coding RNA analysis of muscular responses to testosterone deficiency in Huainan male pigs. Animal science journal = Nihon chikusan Gakkaiho. 2017;88(9):1451–6.
16. Wang J, Ren QL, Hua LS, Chen JF, Zhang JQ, Bai HJ, Li HL, Xu B, Shi ZH, Cao H, Xing BS, Bai XX. Comprehensive Analysis of Differentially Expressed mRNA, lncRNA and circRNA and Their ceRNA Networks in the Longissimus Dorsi Muscle of Two

Different Pig Breeds. Int J Mol Sci. 2019;20(5):1107.

17. Li MZ, Wu HL, Luo ZG, Xia YD, Guan JQ, Wang T, et al. An atlas of DNA methylomes in porcine adipose and muscle tissues. Nat Commun. 2012;3:850.
18. Kim D, Pertea G, Trapnell C, Pimentel H, Kelley R, Salzberg SL. TopHat2: accurate alignment of transcriptomes in the presence of insertions, deletions and gene fusions. Genome biology. 2013;14(4):R36–6.
19. Young MD, Wakefield MJ, Smyth GK, Oshlack A. Gene ontology analysis for RNA-seq: accounting for selection bias. Genome biology. 2010;11(2):R14–4.
20. Mao XZ, Cai T, Olyarchuk JG, Wei LP. Automated genome annotation and pathway identification using the KEGG Orthology (KO) as a controlled vocabulary. Bioinformatics. 2005;21(19):3787–93.
21. Liao BJ, Bao XC, Liu LQ, Feng SP, Zovoilis A, Liu WB, et al. MicroRNA cluster 302–367 enhances somatic cell reprogramming by accelerating a mesenchymal-to-epithelial transition. J Biol Chem. 2011;286(19):17359–64.
22. Livak KJ, Schmittgen TD. Analysis of relative gene expression data using real-time quantitative PCR and the 2(-Delta Delta C(T)) Method. Methods. 2001;25(4):402–8.
23. Chen FF, Xiong Y, Peng Y, Gao Y, Qin J, Chu GY, et al. miR-425-5p Inhibits Differentiation and Proliferation in Porcine Intramuscular Preadipocytes. Int J Mol Sci. 2017;18(10):2101.
24. Wang GQ, Zhu L, Ma ML, Chen XC, Gao Y, Yu TY, et al. Mulberry 1-Deoxynojirimycin Inhibits Adipogenesis by Repression of the ERK/PPARγ Signaling Pathway in Porcine Intramuscular Adipocytes. J Agric Food Chem. 2015;63(27):6212–20.
25. 25. Li MX, Sun XM, Cai HF, Sun YJ, Plath M, Li CJ, et al. Long non-coding RNA ADNCR suppresses adipogenic differentiation by targeting miR-204. Biochim Biophys Acta 2016; 1859 (7): 871–82.
26. Rhoads RP, Baumgard LH, El-Kadi SW, Zhao LD. Physiology And Endocrinology Symposium: Roles for insulin-supported skeletal muscle growth. *Journal of animal science* 2016; 94 (5): 1791–1802.
27. Segalés J, Perdiguero E, Muñoz-Cánoves P. Regulation of Muscle Stem Cell Functions: A Focus on the p38 MAPK Signaling Pathway. Frontiers in cell developmental biology. 2016;4:91–1.
28. Jiao Y, Liang X, Hou J, Aisa Y, Wu H, Zhang Z, et al. Adenovirus type 36 regulates adipose stem cell differentiation and glucolipid metabolism through the PI3K/Akt/FoxO1/PPARγ signaling pathway. Lipids Health Dis. 2019;18(1):70–0.
29. Dong X, Tang S, Zhang W, Gao W, Chen Y. GPR39 activates proliferation and differentiation of porcine intramuscular preadipocytes through targeting the PI3K/AKT cell signaling pathway. J Recept Signal Transduct Res. 2016;36(2):130–8.
30. Liu G, Li M, Xu Y, Wu S, Saeed M, Sun C. ColXV promotes adipocyte differentiation via inhibiting DNA methylation and cAMP/PKA pathway in mice. Oncotarget. 2017;8(36):60135–48.
31. Siengdee P, Trakooljul N, Murani E, Brand B, Schwerin M, Wimmers K, er al. Pre- and post-natal muscle microRNA expression profiles of two pig breeds differing in muscularity. *Gene* 2015; 561 (2): 190–198.
32. He DT, Zou TD, Gai XR, Ma JD, Li MZ, Huang ZQ, et al. MicroRNA expression profiles differ between primary myofiber of lean and obese pig breeds. 2017; 12 (7): e0181897.
33. Cai ZW, Zhang LF, Chen ML, Jiang XL, Xu NY. Castration-induced changes in microRNA expression profiles in subcutaneous adipose tissue of male pigs. J Appl Genet. 2014;55(2):259–66.
34. Prats-Puig A, Ortega FJ, Mercader JM, Moreno-Navarrete JM, Moreno M, Bonet N, et al. Changes in circulating microRNAs are associated with childhood obesity. J Clin Endocrinol Metab. 2013;98(10):E1655–60.
35. Ortega FJ, Moreno-Navarrete JM, Pardo G, Sabater M, Hummel M, Ferrer A, et al. MiRNA expression profile of human subcutaneous adipose and during adipocyte differentiation. PLoS One. 2010;5(2):e9022.
36. Lee JS, Kim JM, Lim KS, Hong JS, Hong KC, Lee YS. Effects of polymorphisms in the porcine microRNA MIR206 / MIR133B cluster on muscle fiber and meat quality traits. Anim Genet. 2013;44(1):101–6.
37. Feng Y, Niu LL, Wei W, Zhang WY, Li XY, Cao JH, et al. A feedback circuit between miR-133 and the ERK1/2 pathway involving an exquisite mechanism for regulating myoblast proliferation and differentiation. Cell Death Dis. 2013;4(11):e934.
38. Liu YK, Li MZ, Ma JD, Zhang J, Zhou CW, Wang T, et al. Identification of differences in microRNA transcriptomes between porcine oxidative and glycolytic skeletal muscles. BMC Mol Biol. 2013;14:7.

39. Sun WQ, Hu SQ, Hu JW, Yang S, Hu B, Qiu JM, et al. miR-365 inhibits duck myoblast proliferation by targeting IGF-I via PI3K/Akt pathway. Biosci Rep. 2019;39(11):BSR20190295.
40. Zhang P, Zheng CY, Ye H, Teng Y, Zheng B, Yang X, et al. MicroRNA-365 inhibits vascular smooth muscle cell proliferation through targeting cyclin D1. Int J Med Sci. 2014;11(8):765–70.
41. Li WY, Liu DL, Tang SQ, Li DH, Han RL, Tian YD, et al. A multiallelic indel in the promoter region of the Cyclin-dependent kinase inhibitor 3 gene is significantly associated with body weight and carcass traits in chickens. Poult Sci. 2019;98(2):556–65.
42. Lozano-Velasco E, Galiano-Torres J, Jodar-Garcia A, Aranega AE, Franco D. miR-27 and miR-125 Distinctly Regulate Muscle-Enriched Transcription Factors in Cardiac and Skeletal Myocytes. *Biomed Res Int*, 2015; 391306.
43. Runfola V, Sebastian S, Dilworth FJ, Gabellini D. Rbfox proteins regulate tissue-specific alternative splicing of Mef2D required for muscle differentiation. J Cell Sci. 2015;128(4):631–7.
44. Chu YX, Yao Y, Zhu YB, Shi XE, Sun SD, Li X. MiR-370 enhances cell cycle and represses lipid accumulation in porcine adipocytes. *Anim Biotechnol* 2019; Dec 3: 1–9.
45. Feng YT, Zhou LT, Peng Y, Yang YC, Fan TY, Jiang X, et al. The Role of miR-326 in Adipogenic Differentiation of Human Adipose-Derived Stem Cells by Targeting C/EBPalpha in vitro. Anat Rec (Hoboken) 2019; Oct 8.
46. Belarbi Y, Mejhert N, Gao H, Arner P, Ryden M, Kulyte A. MicroRNAs-361-5p and miR-574-5p associate with human adipose morphology and regulate EBF1 expression in white adipose tissue. Mol Cell Endocrinol. 2018;472:50–6.
47. Cazanave SC, Mott JL, Elmi NA, Bronk SF, Masuoka HC, Charlton MR, et al. A role for miR-296 in the regulation of lipoapoptosis by targeting PUMA. J Lipid Res. 2011;52(8):1517–25.
48. Guo YT, Zhang XX, Huang WL, Miao XY. Identification and characterization of differentially expressed miRNAs in subcutaneous adipose between Wagyu and Holstein cattle. Sci Rep. 2017;7:44026.
49. Hashemi Gheinani A, Burkhard FC, Rehrauer H, Aquino Fournier C, Monastyrskaya K. MicroRNA MiR-199a-5p regulates smooth muscle cell proliferation and morphology by targeting WNT2 signaling pathway. J Biol Chem. 2015;290(11):7067–86.
50. Zhang H, Zhu SY, Zhang CT, Liu WJ, Zhu JC. miR-199a-5p inhibits the proliferation of rat airway smooth muscle cells and the expression of hypoxia inducible factor 1 alpha under hypoxia conditions. Xi Bao Yu Fen Zi Mian Yi Xue Za Zhi Chinese Journal of Cellular Molecular Immunology. 2015;31(9):1183–8.
51. Alexander MS, Kawahara G, Motohashi N, Casar JC, Eisenberg I, Myers JA, et al. MicroRNA-199a is induced in dystrophic muscle and affects WNT signaling, cell proliferation, and myogenic differentiation. Cell Death Differ. 2013;20(9):1194–208.
52. Yan MJ, Yang SB, Meng FB, Zhao ZH, Tian ZS, Yang P. MicroRNA 199a-5p induces apoptosis by targeting JunB. Sci Rep. 2018;8:6699.
53. Esteves JV, Yonamine CY, Pinto-Junior DC, Gerlinger-Romero F, Enguita FJ, Machado UF. Diabetes Modulates MicroRNAs 29b-3p, 29c-3p, 199a-5p and 532-3p Expression in Muscle: Possible Role in GLUT4 and HK2 Repression. Front Endocrinol (Lausanne). 2018;9:536.
54. Davoli R, Gaffo E, Zappaterra M, Bortoluzzi S. Identification of differentially expressed small RNAs and prediction of target genes in Italian Large White pigs with divergent backfat deposition. 2018; 49 (3): 205–214.
55. Kajimoto K, Naraba H, Iwai N. MicroRNA and 3T3-L1 pre-adipocyte differentiation. Rna. 2006;12(9):1626–32.
56. Laine SK, Alm JJ, Virtanen SP, Aro HT, Laitala-Leinonen TK. MicroRNAs miR-96, miR-124, and miR-199a regulate gene expression in human bone marrow-derived mesenchymal stem cells. J Cell Biochem. 2012;113(8):2687–95.
57. Watanabe T, Sato T, Amano T, Kawamura Y, Kawamura N, Kawaguchi H, et al. Dnm3os, a non-coding RNA, is required for normal growth and skeletal development in mice. Dev Dyn. 2008;237(12):3738–48.
58. Shi XE, Li YF, Jia L, Ji HL, Song ZY, Cheng J, et al. MicroRNA-199a-5p affects porcine preadipocyte proliferation and differentiation. Int J Mol Sci. 2014;15(5):8526–38.
59. Zhang XN, Liu LL, Dou CY, Cheng PP, Liu L, Liu HR, et al. PPAR Gamma-Regulated MicroRNA 199a-5p Underlies Bone Marrow Adiposity in Aplastic Anemia. Molecular therapy Nucleic acids. 2019;17:678–87.
60. Zhao YB, Zhao J, Zhang LJ, Shan RG, Sun ZZ, Wang K, et al. MicroRNA-370 protects against myocardial ischemia/reperfusion injury in mice following sevoflurane anesthetic preconditioning through PLIN5-dependent PPAR signaling pathway. Biomed Pharmacother. 2019;113:108697.

61. Jiao YR, Huang B, Chen Y, Hong GL, Jian X. H CY, et al. Integrated Analyses Reveal Overexpressed Notch1 Promoting Porcine Satellite Cells' Proliferation through Regulating the Cell Cycle. Int J Mol Sci. 2018;19(1):271.
62. Ding HY, Zheng SS, Garcia-Ruiz D, Hou DX, Wei Z, Liao ZC, et al. Fasting induces a subcutaneous-to-visceral fat switch mediated by microRNA-149-3p and suppression of PRDM16. Nat Commun. 2016;7:11533.
63. Yue T, Fang Q, Yin J, Li D, Li DF. W. S-adenosylmethionine stimulates fatty acid metabolism-linked gene expression in porcine muscle satellite cells. Mol Biol Rep. 2010;37(7):3143–9.
64. Cui JX, Chen W, Zeng YQ. Development of FQ-PCR method to determine the level of ADD1 expression in fatty and lean pigs. Genetics Molecular Research. 2015;14(4):13924–31.
65. Munoz M, Garcia-Casco JM, Caraballo C, Fernandez-Barroso MA, Sanchez-Esquiliche F, Gomez F, et al. Identification of Candidate Genes and Regulatory Factors Underlying Intramuscular Fat Content Through Longissimus Dorsi Transcriptome Analyses in Heavy Iberian Pigs. Front Genet. 2018;9:608.
66. Yu KF, Shu G, Yuan FF, Zhu XT, Gao P, Wang SB, et al. Fatty acid and transcriptome profiling of longissimus dorsi muscles between pig breeds differing in meat quality. Int J Biol Sci. 2013;9(1):108–18.
67. Halmos T, Suba I. The physiological role of growth hormone and insulin-like growth factors. Orv Hetil. 2019;160(45):1774–83.
68. Trigatti BL, Anderson RG, Gerber GE. Identification of caveolin-1 as a fatty acid binding protein. Biochem Biophys Res Commun. 1999;255(1):34–9.
69. Pol A, Luetterforst R, Lindsay M, Heino S, Ikonen E, Parton RG. A caveolin dominant negative mutant associates with lipid bodies and induces intracellular cholesterol imbalance. J Cell Biol. 2001;152(5):1057–70.
70. Wang C, Mei YJ, Li L, Mo DL, Zhang H, Tian XG, et al. Molecular characterization and expression analysis of caveolin-1 in pig tissues. Sci China C Life Sci. 2008;51(7):655–61.
71. Razani B, Combs TP, Wang XB, Frank PG, Park DS, Russell RG, et al. Caveolin-1-deficient mice are lean, resistant to diet-induced obesity, and show hypertriglyceridemia with adipocyte abnormalities. J Biol Chem. 2002;277(10):8635–47.
72. Palacios-Ortega S, Varela-Guruceaga M, Algarabel M, Ignacio Milagro F, Alfredo Martinez J, de Miguel C. Effect of TNF-Alpha on Caveolin-1 Expression and Insulin Signaling During Adipocyte Differentiation and in Mature Adipocytes. Cellular Physiology Biochemistry. 2015;36(4):1499–516.
73. Frank PG, Pavlides S, Cheung MWC, Daumer K, Lisanti MP. Role of caveolin-1 in the regulation of lipoprotein metabolism. American journal of physiology Cell physiology. 2008;295(1):C242–8.
74. Frank PG, Cheung MWC, Pavlides S, Llaverias G, Park DS, Lisanti MP. Caveolin-1 and regulation of cellular cholesterol homeostasis. Am J Physiol Heart Circ Physiol. 2006;291(2):H677–86.
75. Ring A, Le Lay S, Pohl J, Verkade P, Stremmel W. Caveolin-1 is required for fatty acid translocase (FAT/CD36) localization and function at the plasma membrane of mouse embryonic fibroblasts. Biochim Biophys Acta. 2006;1761(4):416–23.
76. Wang DX, Pan YQ, Liu B, Dai L. Cav-1 promotes atherosclerosis by activating JNK-associated signaling. Biochem Biophys Res Commun. 2018;503:513–20.

Additional Files

Additional Figure 1. Correlation analysis of lncRNA expression in different samples. (DOCX 207 kb)

Additional Figure 2. Correlation analysis of lncRNA expression in different samples. (DOCX 253 kb)

Additional Figure 3. Validation of expression trends of ten randomly selected lncRNAs (five upregulated and five downregulated at 75 dpc) by qRT-PCR. Note: *GAPDH* used as reference genes, and fold changes calculated using $2^{-\triangle\triangle Ct}$ method (mean ± SD n = 3 * $p < 0.05$,** $p < 0.01$). (DOCX 21 kb)

Additional Table 1. The information of the primers used for real-time qPCR. (XLSX 18 kb)

Additional Table 2. Summary of read mapping to reference porcine genome (susScr3). (XLSX 18 kb)

Additional Table 3. Information of novel lncRNAs. (XLSX 170 kb)

Additional Table 4 The information of the differently expressed lncRNAs(XLSX 328 kb)

Figures

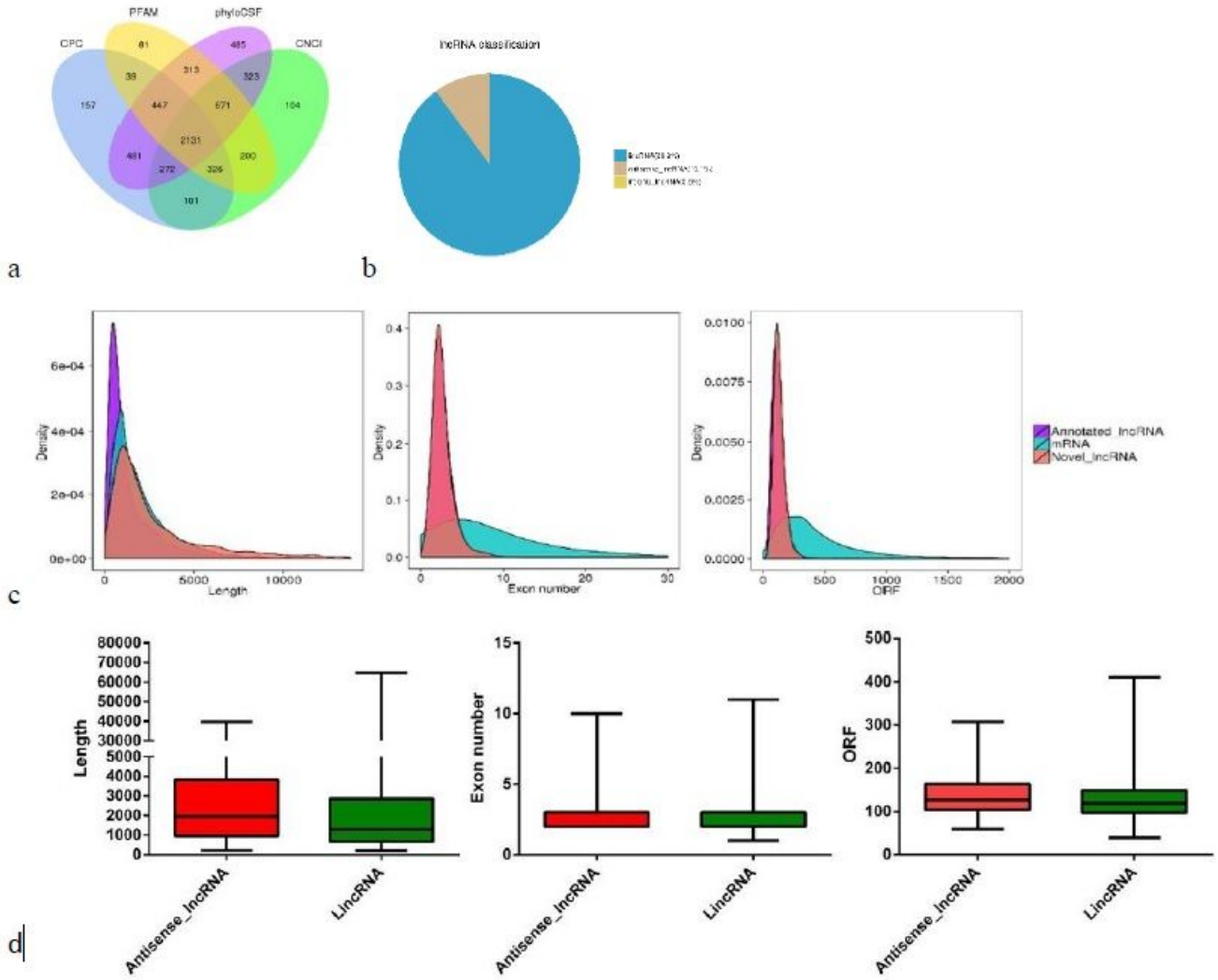

Figure 1

Genomic features of the identified lncRNAs in longissimus dorsi muscle tissue of HN and LW pigs at 35, 55 and 75 days post-conception. a. Screening of candidate lncRNAs by analyzing their coding potential via CPC, CNCI, phyloCSF and PFAM. b. the classification of the 2131 novel identified lncRNAs. c. length, exon number and ORF length distribution of annotated lncRNAs, novel lncRNAs and mRNAs. d. length, exon number and ORF length distribution of novel discovered antisense lncRNAs and lincRNAs.

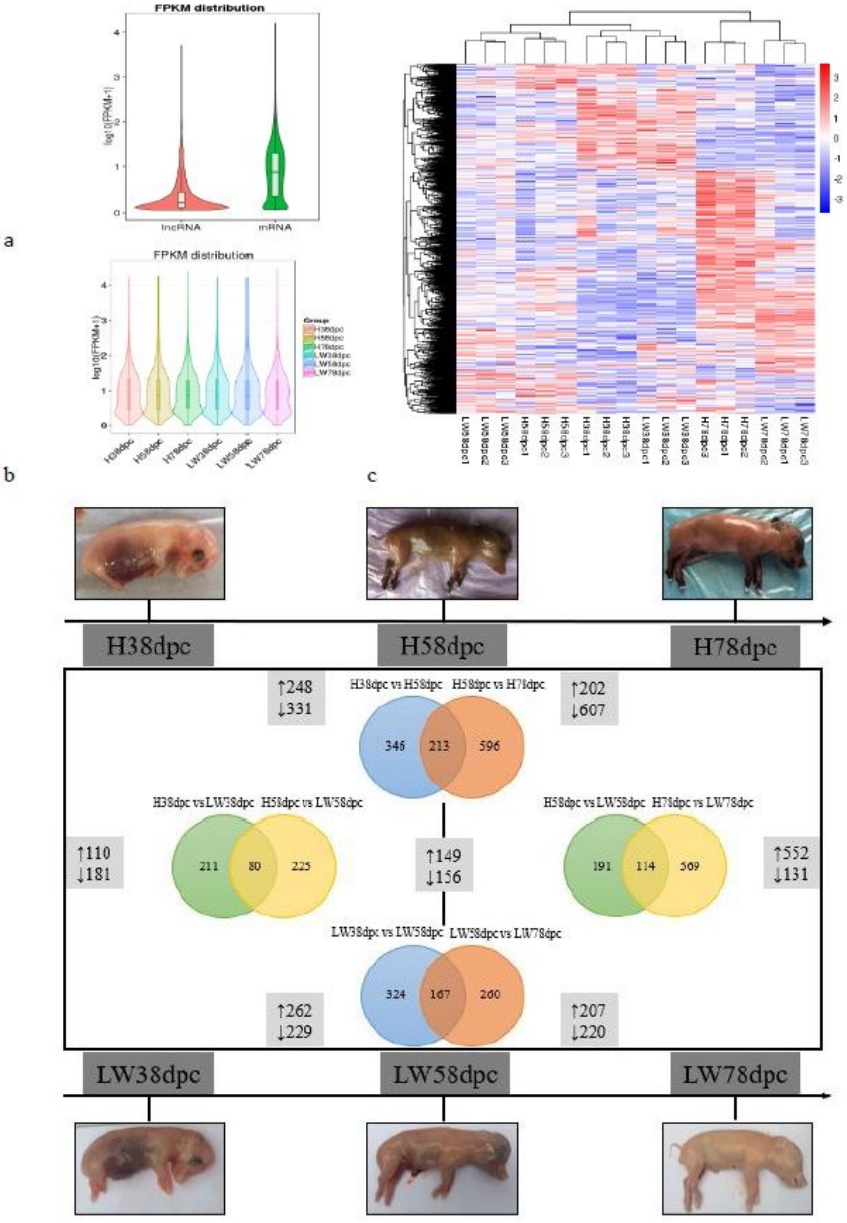

Figure 2

The differentially expressed lncRNAs in longissimus dorsi muscle tissue between Huainan (HN) and Large white (LW) at 38, 58 and 78 post conception. a. The FPKM distribution of lncRNAs and mRNAs. b. The FPKM distribution of lncRNAs in HN and LW. c. H ierarchical clustering of differentially expressed lncRNAs . d. The numbers of DELs between different stages in HN or LW were depicted on vertical lines. The numbers of DELs between HN and LW at each stage were depicted on horizontal lines. represent up regulated, ↓ represent down regulated.

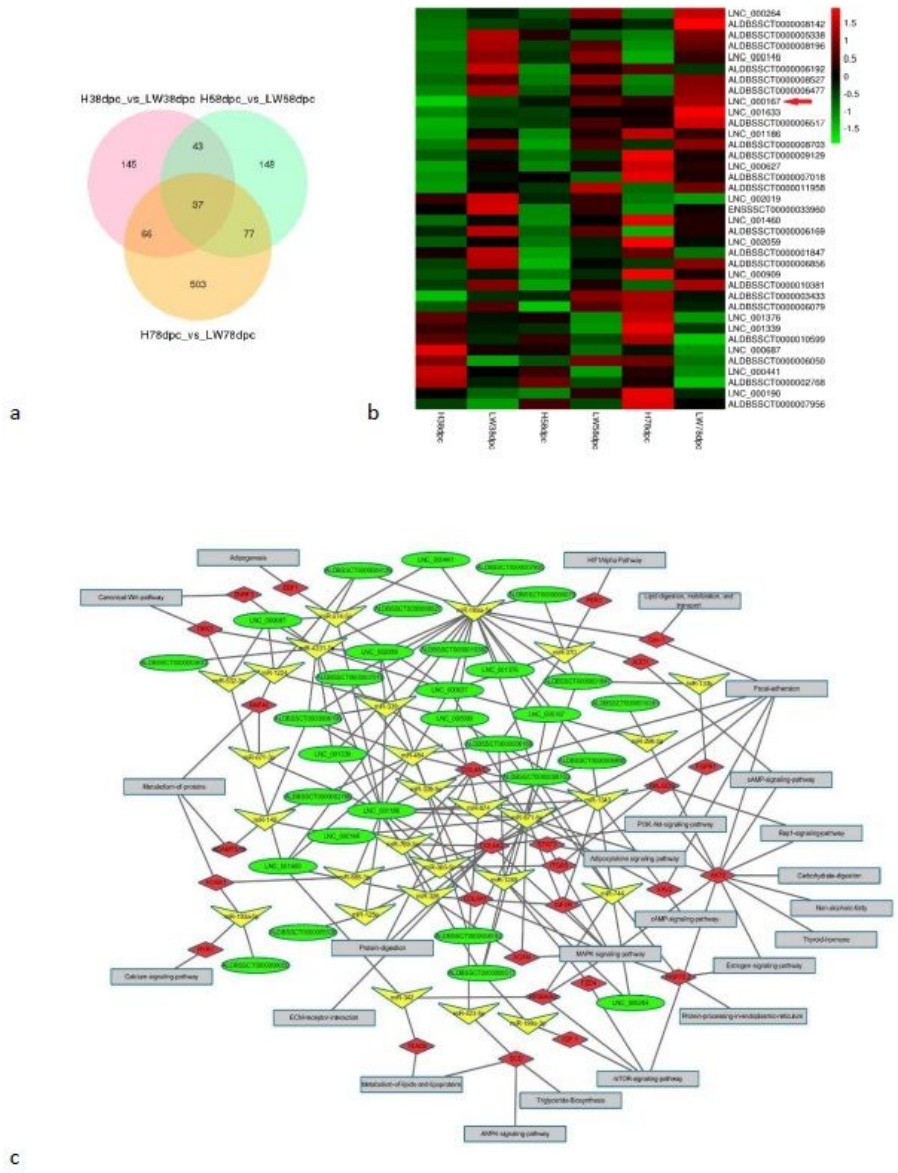

Figure 3

The function of 37 shared DELs between HN and LW at each stage. a. Venn diagram showing the number of overlapping DELs between HN and LW at three stages. b. The heatmaps of the 37 shared DELs' expressional level in three stages between HN and LW pigs. Red arrow showed the selected LNC_000167 (IMFlnc1) c. The ceRNA network of 37 shared DELs. Circular node s represent lncRNAs; triangular nodes represent miRNAs; d iamond nodes represent mRNAs; and square nodes represent pathways

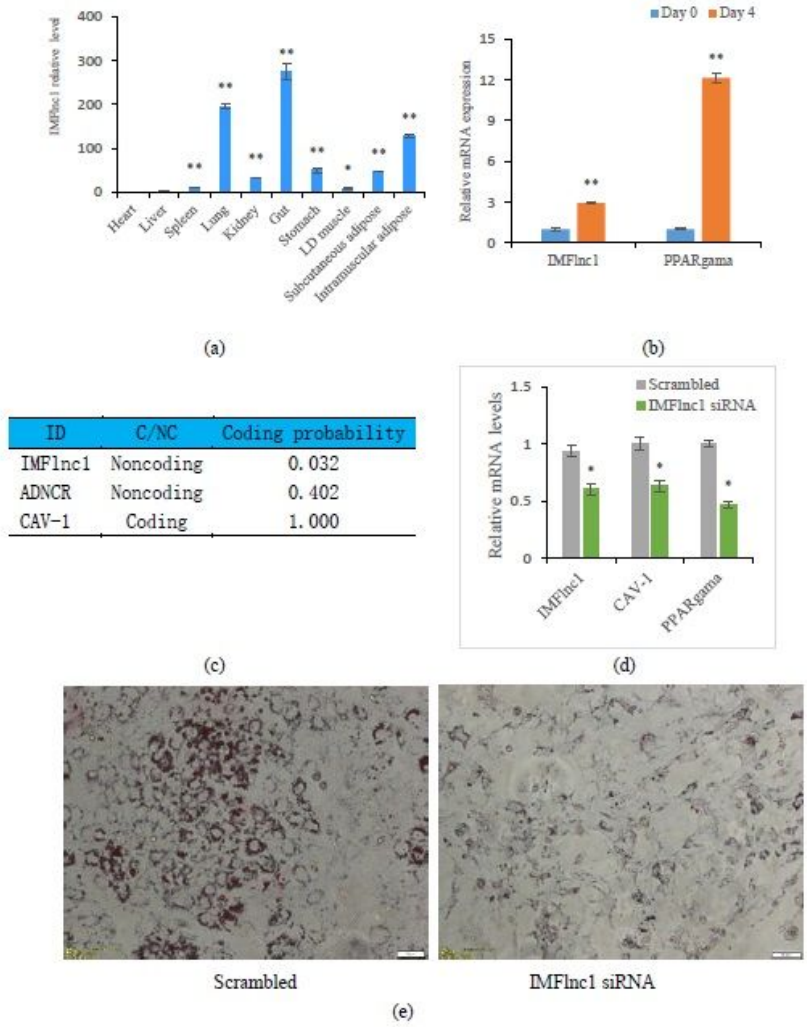

Figure 4

IMFlnc1 was associated with adipogenesis. a. The expression profile of IMFlnc1 in different tissues by qRT PCR. b. The expression level of IMFlnc1 and PPARgama during porcine intramuscular preadipocyte differentiation by qRT PCR. c. The coding probability of IMFlnc1, ADNCR and SIRT1 were analyzed by Coding Potential Calculator 2 (CPC2) program. d. IMFlnc1 siRNA could downregulate expression of IMFlnc1, CAV 1 and PPARgama by qRT PCR. ID C/NC Coding probability IMFlnc1 Noncoding 0.032 ADNCR Noncoding 0.402 CAV-1 Coding 1.000 ** ** ** ** ** * ** ** 0 100 200 300 400 IMFlnc1 r relative ** 0 3 6 9 12 15 IMFlnc1 PPARgama Relative mRNA expression Day 4 * * * 0 0.5 1 1.5 Relative mRNA levels Scrambled IMFlnc1 siRNA e. Inhibition of IMFlnc1 inhibited adipogenesis by Oil Red O staining.

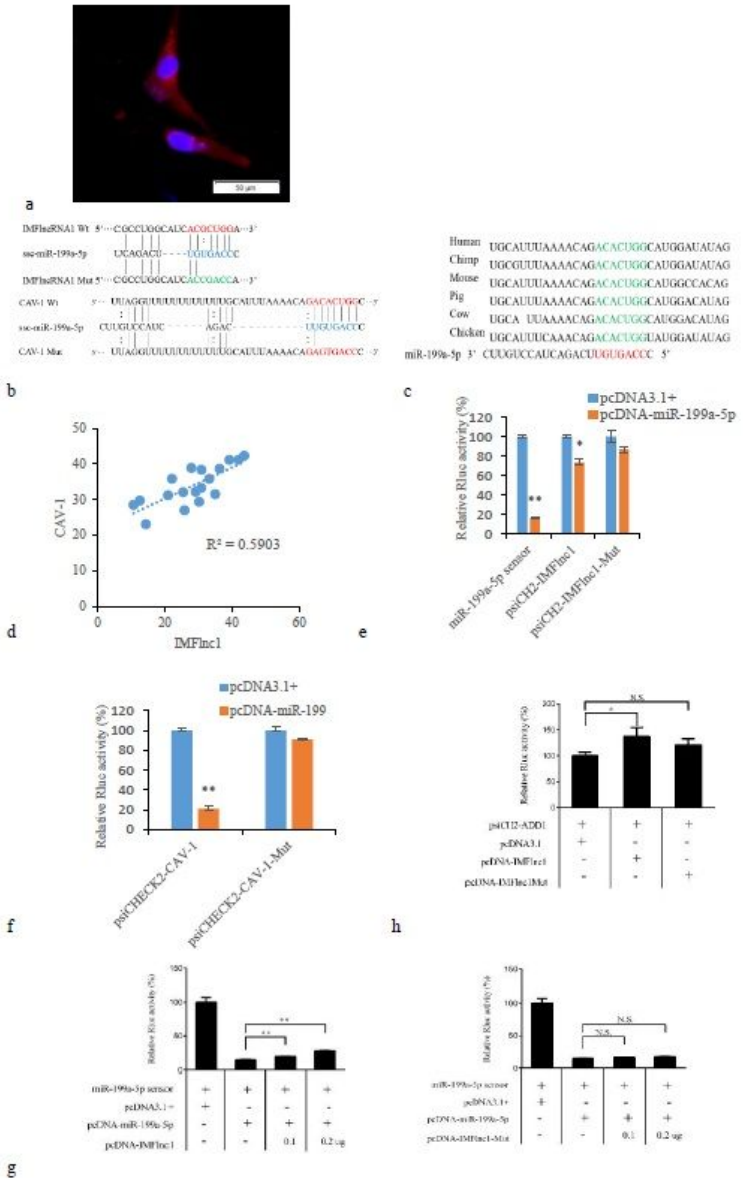

Figure 5

lnc1 regulates CAV 1 expression by sponging miR 199a 5p a. Detection of IMFlnc1 in porcine intramuscular adipocyte by RNA fluorescence in situ hybridization (RNA FISH). Red represents FISH probes of IMFlnc1. Nuclei are counterstained with DAPI (blue). Scale bar, 50 μm. b. The schematic diagram shows the sequences of IMFlnc1 and CAV 1 with miR 199a 5p, inculding wild type (Wt) and mutant type (Mut). c. The binding site of miR 199a 5p at CAV 1 3'UTR (green)are evolutionarily conserved across species. d The correlation analysis of IMFlnc1 expression level and CAV 1 mRNA level in 18 porcine LD muscle tissues. e. IMFlnc1 acted as the target of miR 199a 5p. f. CAV 1 acted as the target of miR 199a 5p g. IMFlnc1 acted as the sponge of miR 199a 5p h. IMFlnc1 increases CAV 1 expression in a miR 199a 5p dependent manner

Supplementary Files

This is a list of supplementary files associated with this preprint. Click to download.

- SupplementaryTable1.TheinformationoftheprimersusedforrealtimeqPCR.docx
- SupplementaryTable2.SummaryofreadsmappingtothereferenceporcinegenomesusScr3..docx
- SupplementaryTable3.TheinformationofnovellncRNAs.xlsx

- Supplementaryfigure.2ThecorrelationanalysisoflncRNAsexpressionindifferentsamples.docx
- SupplementaryTable4.TheinformationofthedifferentlyexpressedlncRNAs.xlsx
- SupplementaryTable4.TheinformationofthedifferentlyexpressedlncRNAs.xlsx
- SupplementaryFig.3ValidationtheexpressiontrendsofthetenrandomlyselectedlncRNAsbyqRTPCR..docx
- SupplementaryFigure1.ThecorrelationanalysisoflncRNAsexpressionindifferentsamples.docx
- SupplementaryTable1.TheinformationoftheprimersusedforrealtimeqPCR.docx
- SupplementaryFigure1.ThecorrelationanalysisoflncRNAsexpressionindifferentsamples.docx
- SupplementaryFig.3ValidationtheexpressiontrendsofthetenrandomlyselectedlncRNAsbyqRTPCR..docx
- Supplementaryfigure.2ThecorrelationanalysisoflncRNAsexpressionindifferentsamples.docx
- SupplementaryTable3.TheinformationofnovellncRNAs.xlsx
- SupplementaryTable2.SummaryofreadsmappingtothereferenceporcinegenomesusScr3..docx